Gravitational collapse and the black hole shadow

Author: Àlex González Fuentes
Facultat de Física, Universitat de Barcelona, Diagonal 645, 08028 Barcelona, Spain.

Advisor: Jaume Garriga Torres

Abstract: We consider a physical scenario of spherically symmetric gravitational collapse involving a domain wall. A static black hole produces a shadow of apparent radius $b_{BHS} = 3\sqrt{3}\ GM$, where M is the black hole mass. Here we analyze how this shadow is generated dynamically. We consider the medium to be transparent and the shadow arising solely from gravitational effects. We discuss this phenomenon quantitatively by studying null geodesics in a dynamical spacetime. Tracing the trajectories of photons we obtain how the distribution of energies varies as a function of time and impact parameter. In the model considered the process of shadow formation takes a time of the order of $\Delta t \sim 40\ GM$.

I. INTRODUCTION

Phase transitions are ubiquitous phenomena in physics, which may give rise to topological defects. The simplest examples of topological defects are domain walls, which result from broken discrete symmetries. These may be relevant for primordial black hole (PBH) formation in the early universe [1]. Here, we consider a scenario in which a spherical domain wall separates two regions of spacetime. By Birkhoff's theorem, the metric outside will be Schwarzschild, while inside it will be Minkowski. The wall will have a surface tension, that will drive its collapse before gravity takes over.

For simplicity, we shall consider this as an isolated system without matter other than the domain wall. Our focus will be on the dynamics of photons in this background.

Our goal will be to study the formation of the black hole shadow that follows from the warping of spacetime. Aside from the Einstein equations determining the background, our basic tool will be the use of conserved quantities implied by the symmetries.

II. SCHWARZSCHILD SOLUTION

It is well-known that, in vacuum, the Schwarzschild solution is the most general metric with spherical symmetry [2].

$$ds^2 = -\Big(1 - \frac{2M}{r}\Big)dt^2 + \frac{1}{\big(1 - \frac{2M}{r}\big)}dr^2 + r^2 d\Omega^2 \ . \quad (1)$$

(We use units where $G = c = 1$). The coefficients of the metric diverge for values $r = 0$ and the Schwarzschild radius $r_S = 2M$, corresponding to the black hole (BH) horizon. However, only $r = 0$ is a physical singularity, since the one at r_S can be avoided by a clever choice of coordinates.

A. Killing vectors

Killing vectors satisfying $\nabla_{(\mu}\xi_{\nu)} = 0$ correspond to spacetime symmetries. As usual, these imply the existence of conserved quantities, so that if K^α is the 4-momentum of a photon, then $K_\alpha \xi^\alpha$ is a constant of motion [2].

In the Schwarzschild metric, two useful Killing vectors are $\xi^\alpha_{(1)} = (\partial_\varphi)^\alpha$ and $\xi^\alpha_{(2)} = (\partial_t)^\alpha$. They lead to conservation of angular momentum and total energy, respectively:

$$\begin{aligned} \xi^\alpha_{(1)} K_\alpha &= K_\varphi = L \ , \\ \xi^\alpha_{(2)} K_\alpha &= K_0 = -E \ . \end{aligned} \quad (2)$$

B. The shadow of a black hole

To be precise about the concept of *shadow*, in this section we study the static BH shadow and afterwards we apply the same definition in the dynamical case. We will consider a setup where every point in spacetime contains a light source that emits in every direction at a certain instant of time $t = 0$. After that, rays follow different paths, but there will not be any additional light source. Therefore, the shadow can be defined as the region from which the observer does not receive light [5].

Massless particles satisfy $g_{\mu\nu}K^\mu K^\nu = 0$, which leads to

$$\left(\frac{dr}{d\lambda}\right)^2 = E^2 - \Big(1 - \frac{2M}{r}\Big)\frac{L^2}{r^2} \ , \quad (3)$$

where λ is an affine parameter. The circular unstable orbits for a photon can be found from the extrema of the effective potential in the right hand side of Eq. (3), resulting in $r_c = 3M$. This is not the same as the radius of the shadow. Instead, we have to use the definition of impact parameter $b \equiv L/E$, consistent with the classical definition in the asymptotic region if we recall that for a photon the linear momentum is equal to the energy. From Eq. (3), one can obtain the impact parameter in

terms of the radius r at the turning point. Note that the apparent radius of the shadow will be determined by the impact parameter for which the turning point is the radius of the unstable orbit, $b(r_c) = 3\sqrt{3}M \equiv b_{BHS}$. At a lower impact parameter, photons fall into the BH.

III. COLLAPSE OF A DOMAIN WALL

A domain wall is characterized by the equation of state $T = \sigma$, where T is the surface tension of the wall and σ the surface energy density [3]. The trajectory of the domain wall is given by $R(\tau)$, where τ is proper time on the wall. For $r < R$ the the metric is Minkowski and for $r > R$ it is Schwarzschild

$$\begin{aligned} ds_-^2 &= -dt^2 + dr^2 + r^2 d\Omega^2 \,, \\ ds_+^2 &= -\Big(1 - \frac{2M}{r}\Big)dt'^2 + \frac{1}{\big(1 - \frac{2M}{r}\big)}dr^2 + r^2 d\Omega^2 \,, \end{aligned} \quad (4)$$

where $d\Omega^2 = d\theta^2 + \sin\theta^2 d\varphi^2$. Without loss of generality, we can fix the geodesic to be equatorial, $\theta = \frac{\pi}{2}$. Unlike the angular coordinates, the radial and temporal coordinate do not follow the same structure inside and outside the wall. Notice, however, that r has a geometric meaning that can be expressed in a coordinate invariant way: it corresponds to the ratio between the proper length of an arc subtending an angle $d\varphi$, and that angle. In other words, it is the proper circumferential radius. By continuity of the metric at the location of the wall $r = R(\tau)$, the circumferential radius must be the same on both sides. Note that this is not the case for the temporal coordinate, and so we use two different names for it, t and t'.

A. Junction conditions

The domain wall has a surface tension that will eventually make it collapse. In order to obtain a dynamical equation for it, a useful tool is to consider junction conditions in the Gauss-Codazzi formalism [4]. As we take the zero-thickness limit, the energy-momentum tensor of the wall requires a Dirac δ distribution $T_{\mu\nu} = S_{\mu\nu}\delta(\eta)$, with $S_{\mu\nu} = -\sigma h_{\mu\nu}$ being interpreted as the energy-momentum tensor restricted to the surface. Here, $h_{\mu\nu} = g_{\mu\nu} - n_\mu n_\nu$ is the metric induced on the wall, with n^μ being the normal vector to the 4-momentum of the wall. Also, we use adapted coordinates $x^\mu \equiv (x^i, \eta)$ with $x^i \equiv (\tau, \theta, \varphi)$ parametrizing points along the surface and η being the proper distance along a normal geodesic from the surface of the wall. It can be shown that the Einstein equations lead to [4]:

$$[K_{ij}] \equiv K_{ij}^S - K_{ij}^M = -4\pi\sigma h_{ij} \,, \quad (5)$$

where $K_{\mu\nu}^{S(M)} = \nabla_{(\mu} n_{\nu)}^{S(M)}$ is the extrinsic curvature as seen from each side of the wall and $n_\mu^{S(M)}$ is outward pointing and different on each side.

In the spacetime we are studying, this junction condition reduces to

$$\beta_M - \beta_S = 4\pi\sigma R = \kappa R \,, \quad (6)$$

where we have labeled $\kappa = 4\pi\sigma$ for convenience and $\beta_{S(M)}$ are defined as:

$$\beta_S = \left(1 - \frac{2M}{R}\right)\dot{t} = \pm\left(1 - \frac{2M}{R} + \dot{R}^2\right)^{1/2} \,, \quad (7)$$

$$\beta_M = \dot{t}' = \pm(1 + \dot{R}^2)^{1/2} \,. \quad (8)$$

Here, the dot means differentiation with respect to the proper time on the surface of the wall τ. By rearranging terms in Eq. (6) and taking the square, we arrive at an expression for $\dot{R}^2$ that only depends on R.

$$\left(\frac{dR}{d\tau}\right)^2 = \frac{2M}{R} - 1 + \left(\frac{2M - \kappa^2 R^3}{2\kappa R^2}\right)^2 \,. \quad (9)$$

This is the equation of motion for the domain wall. As we have argued before, R is continuous on both sides of the wall. Since we are dealing with trajectories that might cross this wall, the optimal strategy for integrating the geodesic equations is to take R as the independent variable. In order to calculate the trajectory of the spherical wall, we can relate $\dot{R}^2$ to the time coordinates outside t and inside t' by means of Eq. (7) and (8) and $(\frac{dR}{dt})^2 = (\frac{dR}{d\tau})^2/(\frac{dt}{d\tau})^2$:

$$\left(\frac{dt}{dR}\right)^2 = \frac{1}{1 - \frac{2M}{R}}\left[1 - \left(1 - \frac{2M}{R}\right)\left(\frac{2\kappa R^2}{2M - \kappa^2 R^3}\right)^2\right]^{-1} \,, \quad (10)$$

$$\left(\frac{dt'}{dR}\right)^2 = 1 - \left[\frac{2M}{R} + \left(\frac{2M - \kappa^2 R^3}{2\kappa R^2}\right)^2\right]^{-1} \,. \quad (11)$$

Note that the sign ambiguity of Eq. (7) and (8) has not disappeared, since the terms are now squared. If we assign an initial radius to the domain wall and impose both time coordinates to start when it begins to collapse, we can integrate the previous equations to establish the evolution of the bubble from both regions: $t(R)$ from Schwarzschild and $t'(R)$ from Minkowski.

B. Continuity conditions

Once the evolution of the wall is determined, we can consider photons emitted at $t = t' = 0$. Our domain wall is not a opaque, so nothing prevents light rays from crossing it. Hence, it is essential to discuss which

quantities remain conserved when we cross from the outside to the inside, and viceversa.

Let K^μ be the 4-momentum of a photon. The geodesic equation of the photon is given by

$$\frac{dK_\mu}{d\lambda} = \frac{1}{2} K^\sigma K^\nu g_{\sigma\nu,\mu} \, . \tag{12}$$

Since the right hand side is not singular (it is discontinuous but it does not have Dirac δ singularities), we can conclude that the vector K_μ is continuous in adapted coordinates. Therefore K_φ is continuous and the angular momentum takes the same value on both sides ($K_{\varphi'} = L' = L = K_\varphi$). For the case of the energy, the consideration is more elaborate, since we use a different temporal coordinate on each side of the wall, adapted to the corresponding temporal Killing vector. When a photon goes through the wall, the tangential and normal projections of K^μ with the surface must be continuous.

$$K^\mu g_{\mu\nu} n^\nu = K^{\mu'} g_{\mu'\nu'} n^{\nu'} \, , \tag{13}$$

$$K^\mu g_{\mu\nu} U^\nu = K^{\mu'} g_{\mu'\nu'} U^{\nu'} \, , \tag{14}$$

where U^μ is the 4-velocity of the wall and n^μ its orthogonal 4-vector. The primed and unprimed expressions refer to the inner an outer regions, respectively. More explicitly, their expression will change depending on the metric of the region.

$$\begin{aligned} U^\mu &= (\dot{t}, \dot{R}) \, , \quad n^\mu = \left(\frac{\dot{R}}{1 - \frac{2M}{R}}, \left[1 - \frac{2M}{R} \right] \dot{t} \right) . \\ U^{\mu'} &= (\dot{t}', \dot{R}) \, , \quad n^{\mu'} = (\dot{R}, \dot{t}') \, . \end{aligned} \tag{15}$$

It becomes clear from this expressions that the angular part of K^μ will play no role in the continuity: the 4-velocity of the wall has only radial and temporal components.

With all this in mind, Eq. (13) and (14) can be employed to determine how the energy of photons emitted at $t = t' = 0$ changes as they cross from one region to the other. Their trajectory might cross the wall twice or once from the time of emission to the time of observation, depending on whether the photon starts inside the bubble or outside. We will use unprimed expressions for a photon emitted in Schwarzschild, primed expressions for this photon entering the bubble and double-primed for the same photon escaping the wall and returning to Schwarzschild. Using $K_0 U^0 + K_r U^r = K_{0'} U^{0'} + K_{r'} U^{r'}$ and substituting $L = Eb$, $L = E'b'$ and $L = E''b''$ where appropriate, we get:

$$\begin{aligned} -\frac{E}{1 - \frac{2M}{R}} \left[\sqrt{1 - \frac{2M}{R} + \dot{R}^2} - \dot{R} \sqrt{1 - \left(1 - \frac{2M}{R} \right) \frac{b^2}{R^2}} \right] = \\ = E' \left[\sqrt{1 + \dot{R}^2} \pm \dot{R} \sqrt{1 - \frac{b'^2}{R^2}} \right] \, , \end{aligned} \tag{16}$$

where we have used $K_{0'} = -E'$ and $K_0 = -E$. Here, $\dot{R}$ represents the motion of the wall, given by Eq. (9). For each crossing we need 2 equations in order to solve for both the new impact parameter and the sign of K_r. The normal projection is $K_0 n^0 + K_r n^r = K_{0'} n^{0'} + K_{r'} n^{r'}$:

$$\begin{aligned} -\frac{E}{1 - \frac{2M}{R}} \left[-\dot{R} - \sqrt{1 - \left(\frac{2M}{R} \right) \frac{b^2}{R^2}} \sqrt{1 - \frac{2M}{R} + \dot{R}^2} \right] = \\ = E' \left[-\dot{R} \pm \dot{R} \sqrt{1 - \frac{b'^2}{R^2}} \sqrt{1 + \dot{R}^2} \right] \, . \end{aligned} \tag{17}$$

The equations for a Minkowski to Schwarzschild crossing can be obtained equivalently. It is essential to choose appropriate values of the parameters κ and the initial radius of the domain wall R_0. We will take r_S as the unit of distance. That implies the units of κ are r_S^{-1}. If we inspect Eq. (10), with $R_0 \gg r_S$ (since we want the bubble to start collapsing far from r_S) and $\kappa \ll R_0$ (because it represents an energy density) in these units:

$$R_0 \sim \left(\frac{r_S}{\kappa} \right)^{1/2} \, . \tag{18}$$

That means the maximum radius is determined by the surface energy density of the bubble.

Another relevant detail is the distance at which we observe the shadow. Ideally, we would want an observer at infinity, but in order to integrate the trajectories, we must set a finite distance. We will set it to be 10 times the size of the shadow of the black hole $b_{BHS} = 3\sqrt{3}M$, where the effects of curvature are negligible. The criteria used for choosing a specific numerical value for κ in TABLE I were that the value of R_0 (determined by Eq. (9) with $\dot{R} = 0$) is big enough to allow some photons to enter and escape the bubble before it collapses.

	Numerical value
$\kappa\,(r_S^{-1})$	0.003
$R_0\,(r_S)$	13.038
$d_\infty\,(r_S)$	25.981

TABLE I: Parameters used for simulations.

The strategy to calculate trajectories will be setting a time at d_∞ and tracing null geodesics backwards:

$$\left(\frac{dr}{dt} \right)^2 = \left[1 - \left(1 - \frac{2M}{r} \right) \frac{b^2}{r^2} \right] \left(1 - \frac{2M}{r} \right)^2 \, .$$

$$\left(\frac{dr}{dt'} \right)^2 = 1 - \frac{b'^2}{r^2} \, . \tag{19}$$

Whenever the trajectory intersects the collapsing bubble, we make use of Eq. (16) and (17) to get the change in energy and continue the evolution until the initial surface

$t = t' = 0$, as can be seen in FIG. 1. For simplicity, we will consider photons emitted at the Tolman-Ehrenfest temperature (which would correspond to global thermal equilibrium in a static gravitational field before the emission of the photons).

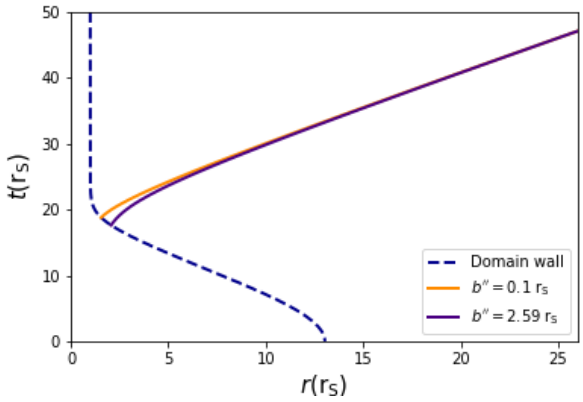

(a) Schwarzschild

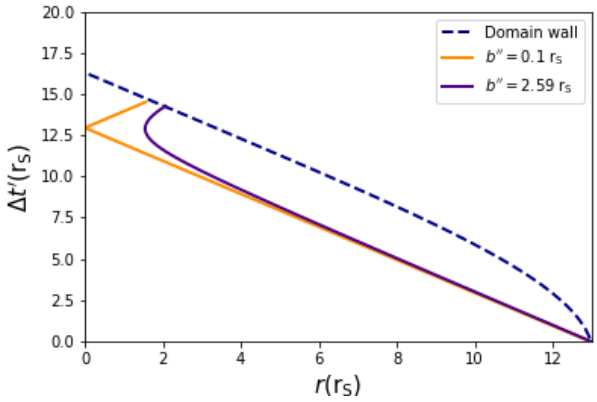

(b) Minkowski

FIG. 1: **a)** Time coordinate as a function of radius of two photons with different impact parameter traced backwards from the observer until the intersection with the bubble. **b)** Time coordinate inside as a function of radius for the same two photons, starting at the instant when they enter the wall. This shows that the domain wall trajectory differs from both perspectives.

IV. RADIAL PHOTONS

First, we can study the simplest case by setting $b = 0$, that is, photons with no angular momentum. This simplifies continuity equations, although they are still crucial to compute the variation in energy.

We can study how a detector at d_∞ receives these photons from the moment the collapse starts until what is left is a BH. In order to establish the range of times of interest, we must integrate Eq. (19) from two characteristic radii until d_∞. The lower bound is defined by the first photon of interest that arrives at the detector, corresponding to the one emitted outwards at R_0. The upper bound, will be determined by the last photon that can escape. However, we know it is not possible to evolve the trajectory from r_S. Such photon is not able to escape the BH until infinite time. Therefore, we must set a minimum radius different from r_S. This can be thought of as setting a minimum energy *cut-off* to trigger our detector. We consider a detector that triggers only when light received has at least a 10% of the original energy of the emitted photons. This corresponds to photons escaping at $r = 1.11\ r_S$. We get $t_\infty(R_0) = 15\ r_S$ and $t_\infty(1.11\ r_S) = 51\ r_S$.

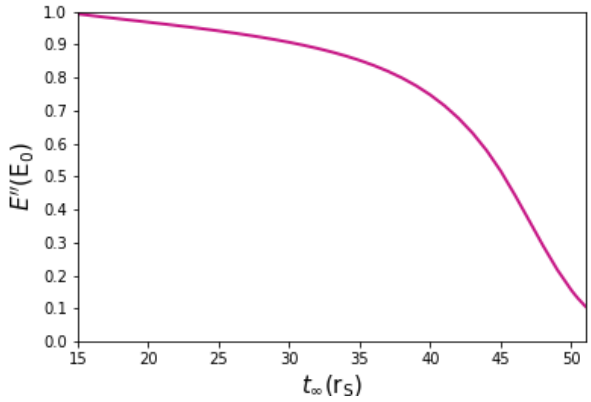

FIG. 2: Energy detected at d_∞ in units of energy emitted in terms of the Schwarzschild time at which they are received.

In FIG. 2 we observe the expected behaviour. It is remarkable that at initial stages of the collapse, photons suffer only a small decrease in energy. It is only for photons escaping near the moment of formation of the BH that the shift becomes increasingly appreciable. This fact can be understood intuitively since photons that cross the surface outwards near r_S appear in a spacetime with extreme curvature.

V. GENERAL CASE

In this section, we will focus on the formation of the BH shadow. We have seen previously that this shadow is defined by $b''_{BHS} = 3\sqrt{3}M$. It can be analyzed by studying how energies vary when considering different impact parameters b''. Photons with different b'' will still be received simultaneously at a certain t_∞. This can be explored for many values of t_∞.

When computing trajectories backwards, a diversity of options should be contemplated. The light ray will arrive at its minimum radius when dr/dt=0 and bounce outwards. If this is achieved before reaching the wall, it must be taken into account by changing the sign in radial velocity and continuing the evolution. If it intersects

the bubble, it is necessary to set $K_r'' < 0$. Nonetheless, depending on the radius at which the change in direction occurs, the photon might not cross the wall. That would mean it was emitted at $t = 0$ outside, so $E'' = E_0$.

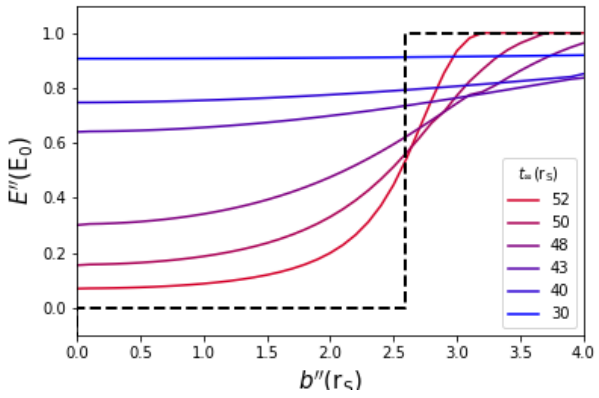

FIG. 3: Energy detected at d_∞ in units of energy E_0 at the time of emission as a function of the impact parameter b'' for different t_∞ in units of the Schwarzschild radius r_S. The dashed profile in black corresponds to the limiting case of a static black hole shadow.

FIG. 3 can be confusing at first glance, but it resembles what should occur:

1. For initial times, the profile approaches a straight line. In fact, if we showed the region with greater b'', it would tend to 1 as expected. The reason for this is that at this stages the domain wall is still huge. Therefore, for a light ray to pass by without entering the bubble, it should have $b \approx R_0$. Furthermore, there exists an energy decrease because photons with lower b'' cross the surface.

2. As time gets closer to the moment at which the domain wall is approximating r_S, the energy distribution approaches the one that constitutes the shadow of a BH. Indeed, it is a step-like distribution since no light is received from the near regions of the BH. All photons with impact parameter greater than b_{BHS} are deflected by the curvature produced by the BH and are detected at d_∞.

VI. CONCLUSIONS

We have analyzed how the black hole shadow is formed dynamically. For this purpose, we have considered the dynamical collapse of a domain wall that divides space in two regions: an inner Minkowskian and an outer Schwarzschild one. By considering the simultaneous emission of photons in every point in space, the tracing of light trajectories backwards has allowed us to obtain, in this simplified model, how the shadow changes.

- For radial photons, we have obtained the profile of energies as a function of time. The result matches what was expected: photons lose a greater amount of energy as the domain wall is closer to r_S, until the BH is formed and no light arrives. The process of darkening for the parameters considered takes a time of the order of $\Delta t_\infty \sim 40\, GM$.

- Photons with angular momentum have been analyzed for different t_∞. It has been shown how the profile expected for the shadow of a BH is recovered as the wall collapses. Once the wall achieves $R = r_S$, the spacetime is indistinguishable from the Schwarzschild solution in the vacuum.

- At the initial stages, a vast region of size $\sim R_0$ loses colour. However, as the wall shrinks, the area that suffers a blackout becomes more localized.

Acknowledgments

I would like to thank my advisor Dr. Jaume Garriga for his help and time invested during the development of this project.

[1] Garriga, J., Vilenkin, A., Zhang, J. (2015). *Black holes and the multiverse.* Journal of Cosmology and Astroparticle Physics, **02**:2016, 064.
[2] Carroll, S. (2019). *Spacetime and Geometry: An Introduction to General Relativity.* Cambridge: Cambridge University Press.
[3] Ipser, J., Sikivie, P. (1984). *Gravitationally repulsive domain wall.* Phys. Rev. D. **30**:712-719.
[4] Blau SK, Guendelman EI, Guth AH. (1987) *Dynamics of false-vacuum bubbles.* Phys. Rev. D Part Fields. 1987 Mar 15;**35**(6): 1747-1766.
[5] Kogan, G., Tsukpo, O., Perlick, V. (2019). *Shadow of black holes at local and cosmological distances.* Proceedings of Science. MULTIF2019. **1910.10514**